LJMU Research Online

Almurshedi, AS, Radwan, M, Omar, S, Alaiya, AA, Badran, MM, Elsaghire, H, Saleem, IY and Hutcheon, GA

 A novel Ph-sensitive liposome to trigger delivery of afatinib to cancer cells: Impact on lung cancer therapy

http://researchonline.ljmu.ac.uk/id/eprint/8334/

Article

For more information please contact researchonline@ljmu.ac.uk

A novel pH-sensitive liposomes to trigger delivery of afatinib to cancer cells: Impact

on lung cancer therapy

Alanood S. Almurshedi, Mahasen Radwan, Samiah Omar, Ayodele A. Alaiya, Mohamed M. Badran, Hanaa Elsaghire, Imran Y. Saleem, Gillian A. Hutcheon.

Abstract

A novel drug delivery systems based on cationic (CL) and pH-sensitive liposomes (PSL) for tyrosine kinase inhibitor afatinib (AFT) were developed to enhance tumor-targetability against NSCLC cells and therapeutic effect. Optimal lipid to drug ratio was selected to prepare AFT-loaded PSL and CL with desirable physiochemical properties based on particle size, drug encapsulation efficiency (EE%), stability and release profiles. Moreover, antitumor activity was performed *in vitro* on human lung cancer cells (H-1975) using a WST-1 assay and Annexin-V apoptosis assay. The mean particle size of the liposomes was less than 100 nm, and EE% was more than 50% with lipid to drug ratio of 1:0.5. Stability data showed that PSL and CL were physically stable for 1 months at 4 and 25 ^{o}C. *In vitro* drug release study demonstrated the sustained release of AFT at pH 7.5; while PSL exhibited fast drug release in pH 5.5. This effect revealed that PSL showed pH-sensitive release behaviors. In addition, the *in vitro* cytotoxicity study was employed for AFT-loaded PSL due to optimal characterizations. Thus, *in vitro* anticancer activity revealed that AFT loaded-PSL triggered apoptosis in H-1975 cells. In addition, the inhibitory effect towards H-1975 and HCC-827 was observed, indicating, which indicated high antitumor activity of AFT-loaded PSL. Then, PSL might potentially create practical clinical strategies for better targetability and delivery of AFT for treatment of lung cancer.

Key words: Afatinib, pH-sensitive liposomes, *In vitro* release, Anticancer activity, Lung cancers

1. Introduction

2

42   Cancer is a foremost problem of disease worldwide to human health in recent years.

43   Moreover, lung cancer becomes a serious danger to human health, it is about 1.38 million

44   cancer-associated mortality in males and females in recent decades [1-2]. The incidence of

45   lung cancer has increased significantly in recent years in Kingdom of Saudi Arabia and

46   United Kingdom due to the increased prevalence of cigarette smoking [3-4].

47   Approximately 85% of lung cancer diagnoses are classified as non-small cell lung cancer

48   (NSCLC) and the remaining 15% small cell lung cancer (SCLC) [6]. The unsatisfactory

49   effects after treatment of lung cancer patients using conventional approaches such as

50   surgical resection, radiation, and chemotherapy were perceived [6]. The majority of

51   chemotherapy administration is intravenous, causing pronounced side effects due to their

52   systemic drug distribution. Moreover, the bioavailability of orally administrated anticancer

53   agents is usually compromised by the first-pass metabolism [7]. The cytotoxic effects of

54   chemotherapeutic agents against normal cells, according to dose-response effects, have

55   been recorded, leading to the patient's frail and death [8]. Therefore, the targeted delivery

56   of anticancer drugs has become a focus of scientific research. NSCLC treatment can be

57   improved by targeted delivery of chemotherapeutic agent (s) to suppress the major

58   signaling pathways involved in lung cancer. Then the targeted delivery of anticancer drugs

59   directly into the lungs can increase their accumulation in tumor cells and reduce adverse

60   side effects [9]. To date, numerous epidermal growth factor (EGFR) targeting agents have

61   been approved, including gefitinib, erlotinib, and lapatinib; however, both primary and

62   acquired resistance are significant clinical problems [10]. Afatinib (AFT) is a novel, potent,

63   small-molecule tyrosine kinase inhibitor (TKI), which is now marketed (2013), as a film-

64   coated oral tablet as a dimaleate salt. AFT is an especially effective treatment for nonsmall

65 cell lung cancer (NSCLC) [11]. AFT has ability to bind covalently and irreversibly to the

66 intracellular TK domain, preventing intracellular signaling [12]. By targeting ErbB family

67 receptors, AFT blocks a wide spectrum of cancer-associated ErbB-driven pathways, and

68 thus has broader antitumor activity against receptors with acquired mutations that are

69 resistant to the first generation of TKIs [13]. AFT exposed at low concentration in the

70 tumor cells, which reduced their clinical uses [14]. Therefore, the targeted delivery of AFT

71 has become a focus of scientific research. Nanomedicine is extensively used due to their

72 intrinsic properties such as improved cancer therapy with reduced toxicity. The

73 nanoparticles may be considered as a promising antitumor delivery system for AFT, which

74 may trigger its delivery to the cancer tissues [15]. The liposomes were the interest type of

75 nanomedicine for clinical application in the field of cancer therapy [16]. In addition, they

76 have ability to target tumor tissues via an enhanced permeation and retention (EPR) effect

77 [15]. Liposomes are suitable carriers for pulmonary drug delivery owing to their capacity

78 for targeting to specific cells/tissues [17]. Although drug-loaded liposomes can extend *in*

79 *vivo* circulation and increase chemotherapeutic activity, they may also be limited targeting

80 and fast cleared [18]. It has been reported that pH-sensitive liposomes have received great

81 attention due to their efficient accumulation in the tumor cells [19]. It has been described

82 that tumor tissues exhibited an acidic condition (pH 5.0-6.5) than normal tissues (pH 7.4-

83 7.5) [20]. Therefore, pH-sensitive liposomes were able to deliver the drugs into the tumor

84 cells when the pH value is lower than the normal tissue. Therefore, it may be expected that

85 pH-sensitive liposomes are more efficient for the delivery of AFT than conventional

86 liposomes due to their fusogenic character [21]. pH-sensitive liposomes could increase the

87 intracellular delivery of their content in cancer cells [20-21]. To the best of our knowledge,

4

88 only one study investigated AFT nanoparticles in term of polymeric micelles as a

89 pulmonary delivery system that improved the therapeutic efficacy in HER2-overexpressed

90 HCT-15-induced tumors [22].

91   In this study, we have prepared three types of liposomes, pH-sensitive liposomes

92 compared with conventional and cationic liposomes containing AFT to study their cancer

93 targeting. An HPLC method was developed and validated for AFT for *in vitro* analysis.

94 The liposomes were characterized in term of particle size distribution, zeta potential and

95 encapsulation efficiency. The surface morphology of the desired liposome was observed

96 by TEM. Moreover, the drug release of AFT was investigated for pH sensitivity (pH 5.5)

97 and prolonged circulation (pH 7.4). The stability studies of these liposomes were

98 performed at a different temperature. Afterward, the NSCLC cells (H-1975 cells) were

99 selected for the assessment of antitumor activity of the optimum liposomes using a

100 colorimetric WST-1 assay and flow cytometry. Moreover, the apoptosis in different cells

101 like H-1975, HCC-827 and H-1650 was established after incubation with liposomes.

102 **2. Materials and methods**

103 2.1. Materials

104   AFT (99.8% purity) was purchased from Green Stone Swiss Co., Limited. 1,2-

105 distearoyl-sn-glycero-3-phosphocholine [18:0] (DSPC), 1,2-dioleoyl-sn-glycero-3-

106 phosphoethanolamine [18:1] (DOPE), 1,2-dioleoyl-sn-glycero-3-phosphocholine [18:1]

107 (DOPC), and 1,2-dioleoy-3-trimethylammonium-propane Chloride salt (DOTAP) were

108 kindly gifted by Avanti Polar Lipid. Cholesteryl hemisuccinate (CHEMS) was purchased

109 from Avanti Polar Lipid. H1975, H-1650, and HCC827 cells were obtained from the

110 American Type Culture Collection (ATCC, Manassas, VA, USA). Cells were maintained

111 at 37°C and 5% CO2 in RPMI 1640 medium (GIBCO®, SIGMA-ALDRICH, Saint Louis,

112 USA) containing 10% fetal bovine serum (FBS) and1% antibiotic/antimycotic which were

113 purchased from (GIBCO®, InvitrogenTM, Carlsbad, USA). All other reagents and

114 chemicals were of analytical grade.

115 **2.2. HPLC assay of AFT**

116 2.2.1. HPLC instrumentation

117 A Water Breeze2^{TM} HPLC system (Waters Corporation, Milford, U.S.A) was used

118 for method development. The HPLC system equipped with an automated sampling system

119 (Waters^{TM} 2695 Plus Autosampler, USA) at 4°C and a photodiode array detector

120 (Waters^{TM} 2998, USA). The HPLC system was examined by "Breeze2 (Water^{TM})"

121 software. AFT was analyzed using mobile phase that consisted of A: 0.1% triethanolamine

122 and 1% acetonitrile in HPLC water (pH= 6), and B: acetonitrile and 10% methanol at a

123 flow rate of 1 mL/min. The mobile phase flowed over a reversed-phase C18 column

124 (Water^{TM}, 3 x 150 mm, 3.5 µm particle size) coupled with a C18 guard cartridge (4×2.0

125 mm) and maintained at 50 °C. The injection volume of each AFT sample was 10 µl and

126 detected by the UV detector at 253 nm. All the operations were carried out at room

127 temperature.

128 2.2.2. HPLC assay

129 A stock solution of AFT was prepared in methanol at a concentration of 1 mg/ml

130 and stored in 4.0 ml amber glass vials at -20°C. Serial dilutions in mobile phase were

131 performed in the range of 0.01 to 25 µg/ml to produce a standard calibration curve and

132 stored at -20°C. A daily standard calibration curve (n=3) ranging from 0.01 to 25 µg/ml

was prepared to determine the unknown AFT concentrations for entrapment efficiency and drug release.

2.2.3. Method validation

The validation of HPLC method was conducted according to the International Conference on Harmonization (ICH) guidelines. The following items were considered for validation: linearity, accuracy, precision, specificity, limit of detection (LOD), limit of quantification (LOQ) and robustness. Three standard calibration lines were prepared at different times (3 months) to evaluate the linearity, precision, accuracy, and stability of the method.

Linearity was assessed by calculating a regression line by plotting the peak area of AFT vs. the AFT concentration ranging from 0.01 to 25 µg/ml. The accuracy was determined via the analysis of multiple replicates (n = 6) of AFT concentration. The accuracy of the method was expressed in term of bias.

The precision of a quantitative method was determined by repeatability as intra-day precision by an analysis of three replicates of AFT concentrations over the same day. Inter-day precision was determined by the analysis of three replicates of various AFT concentrations over three different days. The results were expressed as the relative standard deviation (RSD%).

Low, medium, and high concentration quality control (QC) samples at concentrations of (100, 1,000 and 10,000 ng/ml AFT, respectively) were analyzed, on three distinct occasions within at least 3 months, as before described.

The LOD and LOQ were determined from the calibration curve obtained using six replicates that were closest to the LOQ. The following equations were used:

$$LOD = 3.3 \, \sigma/S \qquad\qquad\qquad \text{Eq. 1}$$

$$LOQ = 10 \, \sigma/S \qquad\qquad\qquad \text{Eq. 2}$$

LOD and LOQ were determined based upon the slope (S) of the calibration curve and least standard deviation obtained from the response (σ). It has a low limit of quantitation (5 ng/ml) with satisfactory specificity, no matrix interference was observed. These findings demonstrated that the assay has good selectivity.

2.3. Preparation of liposomes

Different types of AFT-loaded liposomes were fabricated by thin-film hydration method followed by extrusion as described previously [23]. Non-targeting liposomes (NL) were prepared using DSPC, DOPC, and DOPE at molar ratios of 3: 3: 10. Moreover, three parts of the 10 parts of DOPC of the total liposomal contents were replaced by DOTAP or CHEMS to form cationic and pH-sensitive liposomes, respectively. The AFT was added to the lipids at ratios of 0.25:1, 0.5:1, 0.75:1, 1:1, 1.25:1 and 1.5:1 (w:w), respectively. The composition of the liposomes was presented in Table 1. Briefly, AFT and lipids were dissolved in chloroform, in a round bottom flask following by evaporation to obtain dried thin film at 55 °C using a rotary evaporator (Buchi Rotavapor R-200, Switzerland). The resulting lipid film was hydrated with the proper volume of phosphate buffer saline (PBS; pH 7.4) by gently mixing for 30 min at 55 °C to produce multilamellar vesicles (MLVs). The liposomes were subjected to extrusion through polycarbonate membranes with two pore sizes (200 and 100 mm) using a discontinuous extruder (Liposo-Fast™ Avestin Inc., Ottawa, Canada). The liposomes were extruded 5 times through a polycarbonate membrane with a pore size of 200 nm following by 21 times through 100 nm at low pressure (200 psi). The three types of plain liposomes were prepared similarly. The final formulations were stored for overnight at 4°C.

2.4. Physicochemical characterization of liposomes

2.4.1. Particles size distribution and zeta potential

The mean vesicle sizes, size distribution and the zeta potential (ζ) were characterized by dynamic light scattering (DLS) at 25 $^{\circ}$C with a fixed angle of 137° using a Zetasizer Nano ZS (Malvern Instruments Ltd., UK). The liposomes were appropriately diluted with purified and filtered water (0.2 μm pore size) prior to the measurements. The mean vesicle diameters were the averages of five measurements. All measurements were done in triplicate.

2.4.2. Encapsulation efficiency

Due to the poor solubility of AFT, the free AFT occurred in two forms in the external phase of the liposomal dispersion like free undissolved and free dissolved AFT. The free undissolved AFT was separated from the liposomes using light centrifugation. Meanwhile, the supernatant (encapsulated and free dissolved AFT) were filled into centrifuge tubes and ultra-centrifuged at 40000 rpm at 4 ∘C. The clear supernatant which contained the free dissolved AFT was collected. The total AFT regard to the sum of both encapsulated and free AFT that is existed in the liposomal preparation. The concentration of total AFT was determined after dissolving and disrupting of the liposomal dispersion in methanol and triton x-100 using a vortex mixer, followed by centrifugation for 15 min. The clear supernatant which contained the total AFT was then transferred to a new tube and kept at 4 ∘C until analysis.

The drug encapsulation efficiency (EE%) was calculated using the total drug content of liposomal (AFT$_{total}$) dispersion and un-entrapped drug content of the dispersion (AFT$_{free}$). The EE% of all the formulation was calculated by using the following formula:

204
$$EE\% = \frac{AFT_{total} - AFT_{free}}{AFT_{toal}} \times 100 \qquad \text{Eq. 3}$$

205   2.4.3. Morphology of liposomes

206   The morphology of selected liposomes was visualized by transmission electron

207   microscope (TEM) using a JEM-2100 electron microscope (Jeol, Tokyo, Japan). Briefly, a

208   drop of diluted liposomes was applied to a copper grid and the excess liquid was removed

209   using filter paper. The samples were air-dried for 15 min and observed by TEM.

210   2.4.4. Stability study

211   The physical stability of the selected liposomes was conducted to monitor the

212   physical stability of AFT loaded liposome formulations (Table 2). All liposomal

213   formulations were stored in glass vials at 4±1 °C and 25°C ± 2°C for a period of one month.

214   The stability was evaluated by measuring the average particle size, ζ and PDI during the

215   storage. The AFT content was evaluated by HPLC. The physicochemical stability of the

216   freshly prepared formulation (at day1) was used as the control and the AFT content on day

217   1 was normalized to 100%.

218   2.4.5. *In vitro* drug release

219   *In vitro* release profile of AFT from of NL, CL, and PSL (selected liposomes) were

220   evaluated using the Franz diffusion cell system (FDC-6, LOGAN, Instruments

221   Corporation, USA). The experiments were conducted in 7 ml of PBS buffer (pH 7.4 and

222   5.5) with 0.2% Tween 80 to maintain sink condition. The cellophane dialysis membranes

223   (molecular weight cut off: 12-14 KDa) were soaked before use in distilled water at room

224   temperature for 12 h prior to use to ensure its wetting. An aliquot of 100 μL liposomes was

225   added into donor chambers, ensuring there were no air bubbles under the membrane. The

226   receptor compartment consisted of PBS at pH 7.4 for all liposomes and pH 5.5 for PSL at

227   37 °C, and stirring at 150 rpm. Samples of 500 μL were withdrawn at various time intervals

228   up to 24 h, and replaced immediately with the equal volume of fresh re-heated PBS. The

229   amount of AFT in each sample was analyzed by HPLC. The experiments were performed

230   in triplicate. The data of *in vitro* AFT release were fitted to various kinetic equations,

231   including zero order, first order, Higuchi's model and Korsmeyer Peppas plot and R^2.

232   Then, n values (diffusion exponent) were calculated for each linear curve obtained by the

233   regression analysis of each kinetic equation [24].

2.5. Antitumor activity studies

2.5.1. Cell proliferation assay, WST-1

236   The *in vitro* cytotoxicity of AFT compared to different chemotherapeutic agents

237   (carboplatin, gemacitabine and paclitaxel) was determined using WST-1 using NSCLC

238   cells (H-1975 cells). In brief, the cells were seeded into 96-well plates at a density of 10^4

239   cells/well and incubated overnight in culture medium. Afterward, different concentrations

240   of 1, 5, 10, 20, 40 and 80 μM were added to each well and incubated for additional 24 h.

241   At the end of the treatment, a 10 μl of cell proliferation reagent WST-1 kit was added and

242   incubated for 4 h at 37 °C. The intensities of photometric metabolite (formazan) were

243   measured at 450 nm using an xMark™ Microplate Absorbance Spectrophotometer (Bio-

244   Rad Laboratories, Inc., Hercules, CA, USA). The results are expressed as the IC50, which

245   was obtained graphically using SigmaPlot 10 (SYSTAT Software, Inc., San Diego CA,

246   USA).

2.5.2. Annexin-V apoptosis assay

248   Cell death was assessed using the Vybrant® Apoptosis Assay kit and flow

249   cytometry. The H-1975 cells were seeded in six-well plates at 7 x 10^4 per well and

250   incubated overnight. Then, the cells were treated with pure AFT (control) and AFT loaded

251   PSL at concentrations of 0.5, 1, 3, 5 and 8 μm for 24 h after dilution with culture medium.

252   After treatment, the cells were harvested by trypsinization and centrifuged, and re-

253   suspended in PBS. The cells were stained with Alexa Fluor® 488 Annexin V/propidium

254   iodide (PI) and analyzed using the flow cytometer. The percentage of cell death was

255   determined using FACS-Calibur™ apparatus and CellQuest Pro software (Becton-

256   Dikinson Biosciences, Franklin Lakes. NJ, USA). Moreover, the apoptosis in different cells

257   like H-1975, HCC-827 and H-1650 was tested after application of NL, CL and PSL at 0.25,

258   0.5, 0.75, 1 and 2 µM. Furthermore, the percentage of cell death in the wells containing

259   the free drug and PSL following a 48 and 72h incubation period was subsequently

260   compared with the results of 24 h incubation at 0.25, 0.5, 0.75, 1 and 2 µM.

261   **2.6. Statistical analysis**

262   Quantitative data were expressed as the mean ± SD of at least three replicates. The

263   Student's *t*-test and one-way analysis of variance (ANOVA) using IBMSPSS Statistics 21

264   was used to assess multiple comparisons between different methods and times. The level

265   of confidence was set as 95%.

266   **3. Results**

267   3.1. HPLC assay

268   Three HPLC methods have been described for AFT quantification in dosage forms

269   [25]. This method has been reported by Vejendle *et al*, which demonstrated a lack of

270   sensitivity with LOD (60 ng/ml) and a longer run time (20 min). Therefore, A new sensitive

271   HPLC method for AFT analysis was developed in the current study. This method was used

272   to quantify the AFT concentration for its *in vitro* studies. The method was determined to

273   be specific for AFT in the matrix with no interfering peaks.

274   It was identified in our laboratory that the maximum absorbance for AFT is at 206

275   and 253 nm. While, the HPLC analytical methods reported in the literature detected AFT

276   at 252, 258 or 268 nm. Therefore, the detection wavelength of 253 nm was used for a better

277   sense of AFT in the HPLC in this study. As shown in Fig. 1, the average retention time

278   was 2.4 min, with no interfering peaks in chromatogram A (the blank) and chromatograms

279   B, C (AFT). The obtained results indicated the specificity of the HPLC assay method. It

280   should be mentioned that, during the *in vitro* studies, there was no interfering peaks from

281   the NP ingredients co-eluted with the AFT peak, which further confirmed the specificity

282   of the method.

283   3.2. Method validation

284   A calibration curve of the peak area of AFT vs. the various AFT concentrations, in

285   the range of 0.01 to 25 µg/ml was conducted. The regression equation of the line was

286   obtained ($y = 360232x + 56.95$) resulting in the correlation coefficient (R^2) of 0.9999. The

287   results indicated the quality of the curve (data not shown). Therefore, there was a good

288   linear relationship between the AFT peak area and its tested concentrations.

289   The analytical method was validated in terms of linearity, precision, and accuracy.

290   Linearity was assessed using a calibration curve to investigate the ability of this method to

291   get a proportional response to the different concentrations. Based on the concentrations

292   used ranged from 10 to 250000 ng/m, in triplicate, the linearity was evaluated and a

293   calibration curve was constructed.

294   The LOD was determined to be 10 ng/ml and the LOQ was 5 ng/ml, with the

295   corresponding CV values of 1.8 and 0.93 %, respectively (Table 2).

296   For precision and accuracy of sample analysis, AFT standard solutions of three

297   replicates were prepared in triplicate, and analyzed on the same day (repeatability) or in

298   three different days (intermediate precision). Tables 3 showed that the precision did not

299   exceed the required RSD value with maximum RSD value was < 1.98 %. Analysis of

300   variance of the data indicated no significant difference (p =0.401) in the slopes, intra- and

301   inter-day of the calibration curves. The results confirmed the reproducibility of the assay.

302   The accuracy was more than 99.9 %.

303   The method was found to be robust, since small variations in the method conditions

304   had a negligible effect on the chromatographic behavior of the AFT. The results indicated

305   that changing of the HPLC system or the C_{18} column had no effect on the chromatographic

306   behavior of AFT. Even a small change in the mobile phase composition did not

307   significantly change the peak area of the drug used for this method.

308   3.3. Particle size distribution and zeta potential

309   This study aims to evaluate the incorporation of AFT to CL and PSL compared to

310   NL (control liposomes) for the design of an efficient anticancer delivery system. The

311   obtained liposomes were characterized in terms of the mean particle size, PDI and ζ values

312   using DLS and electrophoretic light scattering (Data not shown). The particle size of the

313   liposomes were ranged from 46 to 57 nm and values of PDI were less than 0.2, which

314   indicate narrower size distribution indicating no aggregation. Regarding ζ, the liposomes

315   presented high values according to the increasing lipid to the drug ratios, until the ratio was

316   1:0.5 (Fig. 2). The AFT-containing liposomes exhibited more positive ζ than liposomes

317 without AFT, which proposes that the addition of DOTAP increased the amounts of AFT

318 in the liposomes. In case of NL, the positive ζ was low and after the incorporation of the

319 drug, ζ increased by approximately two-fold until 1:0.5 of lipid to the drug ratio. CL

320 possessed great values of positive ζ ranging from 38.9 mV for the blank to 48.4 mV for the

321 ratio of 1:0.5. However, PSL exhibited negative values of ζ, due to CHEMS and decreased

322 with the increasing the drug to lipid ratios (Fig. 2).

323 3.4. Encapsulation efficiency

324 The effect of the lipid to drug ratio on the encapsulation of AFT is indicated in Fig.

325 3. As the lipid to AFT ratios increased, the amount of the drug was increased to a certain

326 extent and then decreased. The highest values of the encapsulated AFT were on lipid to

327 drug ratio, 1:0.5, the EE values were 43, 50, and 52 % for NL, PSL, and CL respectively.

328 As expected, the amount of AFT in the liposomes would increase with increasing of drug

329 concentration. After reaching the maximum capacity of AFT, EE values were decreased

330 with more AFT. However, the amount of free drug increased ($P< 0.05$) significantly,

331 thereby notably decreasing the EE%.

332 According to the obtained results, a lipid to drug ratio 1:0.5 in all tested liposomes

333 was selected for further studies due to the high value of EE%. On the contrary, PSL at a

334 lipid to drug ratio of 1:1 showed the lowest EE%.

335 3.5. Morphology of liposomes

336 TEM images of PSL are presented in Fig 4. The images showed that PSL were a

337 spherical shape. In addition, the existence of multilamellar structure was well visualized

338 inside PSL (Fig. 4). It has been reported that the protonated CHEMS showed a lower

339 hydration ability than CHEMS at neutral pH, while the protonated amino group of

340 phosphatidylethanolamine (PE) exhibited greater hydration ability, thus enhancing the

341 immiscibility between PE and CHEMS and causing formation of a heterogeneous system

342 [23].

343 3.6. Stability study

344 The short-term stability of the selected liposomes of lipid:drug ratio of 1:0.5 was

345 investigated for up to 30 days at 4 ± 1 $^{\circ}$C and 25 ± 2 $^{\circ}$C. This ratio was chosen due to the

346 highest EE% of AFT. There was no significant change in the particle size, PDI, ζ and AFT

347 EE% of liposomes during the stability study at 4°C compared to the initial preparation (p

348 > 0.05). However, at 25 $^{\circ}$C, the particle size of the liposomes after storage for 30 days as

349 47.5 ± 2.3 to 75 ± 3.3 nm, 53.8 ± 2.6 to 84 ± 15.9 nm and 55.3 ± 1.2 to 79.5 ± 2.5 for CL, PSL and

350 NL respectively. However, liposomes were still smaller than 100 nm. There was no

351 appreciable change in PDI over 30 days. The ζ at 4°C and 25°C for 30 days exhibited

352 insignificantly different (p =0.141) compared to the initial formulation. The EE% of AFT

353 after storage at 4°C and 25°C for 30 days was slightly decreased but was still higher than

354 90% and 80%, respectively, of the initial formulations (Fig.5).

355 3.7. *In vitro* release study

356 To evaluate the *in vitro* drug release behaviors of AFT from CL and PSL compared

357 to NL, these nanoliposomes were incubated in pH 7.4 PBS solutions at 37 $^{\circ}$C in (Fig. 6).

358 Moreover, to determine the pH sensitivity of PSL, the drug release behavior under pH 5.5

359 was also investigated, and pH 5.5 was selected to mimic the tumor pH (Fig. 6). As weakly

360 acidic environments are presented in the endosomal and lysosomal of tumor cells [26].

361 The AFT release rate was relatively slow in neutral pH 7.4, just reaching 63.6%,

362 28.1% and 35.6 % for CL, NL, and PSL, respectively within 24 h. These data revealed that

363   the liposomes exhibited significantly constant release profiles and AFT was successfully

364   loaded into the liposomes. However, the cumulative release of AFT in PSL at pH 5.5

365   reached to 101 % in 4 h, presenting a burst release phenomenon. The release profiles of

366   AFT from different liposomes apparently biphasic release processes, where rapid release

367   of the surface-adsorbed AFT was observed during the initial phase (first 4 h), followed by

368   a slow release profile for up to 24 h. The AFT release was increased significantly with the

369   pH decreased from 7.4 to 5.5 in case of PSL, and showed reasonably good pH-

370   responsiveness. But, in a physiological environment (pH 7.4), the encapsulated AFT was

371   released at a constant rate. It indicated that the AFT was well protected inside the liposome

372   bilayers at physiological pH. But in acidic condition (pH 5.5) cancer environment, the AFT

373   release was hastened. Therefore, the release of the PSL containing AFT was controlled by

374   the environmental pH. This phenomenon are consistent with the obtained results of

375   doxorubicin release at various pH values [27]. The constant release rate of AFT may

376   conserve a constant contact of the drug to the cancer cell resulted in improved antitumor

377   activity and helpful for drug delivery applications. The PSL system has the greatest

378   potential to improve cancer therapy efficacy. To fit the release kinetics of AFT from

379   liposomes at pH 5.5 and 7.4, different kinetic models viz. Peppas, Higuchi, zero order and

380   first order were exploited to predict the drug release profile. These models depend on the

381   diffusion equations, which based on the composition of liposomes and release conditions.

382   It was reported that the release of the drug from liposomes could be allocated in three

383   different mechanisms: diffusion, erosion and diffusion-erosion [28]. It was found that the

384   results were supported by the Korsmeyer-Peppas model at pH 7.4, which it presented the

385   highest value of R^2. Moreover, the values of n are 0.460, 0.681, 0.431 and 0.599 for CL,

NL, PSL and PSL (pH 5.5), respectively, indicated a non-Fickian diffusion kinetics (0.5 < n < 1) [28]. PSL (n=0.431) exposed Fickian diffusion due to slow release at neutral condition [28]. Subsequently, it is concluded that the drug release mechanism was mainly owing to the combination of diffusion and erosion of the liposomes containing AFT (Table 4).

Moreover, the release profiles of the three AFT-loaded liposomes could be divided into two phases, the first phase from 1 to 4 h and the second phase from 6 and 24 h. The fitting parameters derived from korsmeyer-Peppas were listed in Table 5. n is the release exponent indicating the drug release mechanism and k reflected the rate constant of the release. At pH 7.4, n values of liposomes in the first phase were higher than 0.43, indicating the release behavior of AFT followed a combination of diffusion and erosion control. In the second stage, n values of liposomes were below 0.43, except NL, representing a combination of diffusion and erosion mechanism. The k values for PSL at pH5.5 were much higher than those of pH 7.4, demonstrating the highest release rate in an acidic environment. The difference between k values of the first and second stage were nearly the same, which indicated that the AFT release rate was comparatively slow in a neutral environment.

3.8. Cell proliferation assay, WST-1

In general, it is essential to screen and confirm that the antitumor drugs are potent and efficient for cancer therapy. Therefore, the potency of AFT was evaluated in comparison with selected drugs depending on their activities against lung cancer in an *in vitro* cell-based assay. Half-maximal inhibitory concentration (IC_{50}) of these drugs was

409 attained from an experimentally derived dose-response curve. In this study the cytotoxicity

410 was evaluated with a WST-1 assay in H-1975 cells. The cells were incubated with AFT,

411 paclitaxel, carboplatin and gemcitabine for 24 h. As shown in Fig. 7, the results detected

412 that effect of AFT and paclitaxel on H-1975 cells had dose-dependent manner. On the

413 contrary, the data displayed minor cytotoxicity against H-1975 cells, even up to the highest

414 doses of carboplatin and gemcitabine. The IC_{50} values for AFT and paclitaxel were 20 and

415 25 µM, respectively. Particularly, by increasing the concentrations of AFT to 40 µM, H-

416 1975 cells exhibited higher sensitivity than paclitaxel. The cell viability dropped to 2%

417 with 40 µM of AFT and 50% with paclitaxel. Further increasing the concentration of AFT

418 up to 80 µM, the insignificant reduction in the cell viability was observed (Fig. 7). Thus,

419 *in vitro* anticancer activity revealed that AFT had potent cytotoxic (IC50 value; 20 µM) as

420 compared to other drugs.

421 The cell toxicity of the best liposomes PSL, NL, and CL was also measured by a

422 WST-1 assay on H-1975 cells (data not shown). Unfortunately, the reduction of cell

423 viability (H-1975 cells) at any AFT concentrations did not recorded. This behavior

424 confirmed that the WST-1 assay failed to detect any reduction in viable cell numbers. In

425 contrast, the cytotoxicity (dose-dependent) was detected by microscopic examination using

426 1-80 µM of PSL, NL, and CL. Accordingly, the intracellular vacuoles and cell aggregates

427 at concentrations from 1 to 5 µM was appeared. Further increasing the concentrations from

428 10 to 80 µM, indefinite aggregates of damaged and dying cells were perceived. The order

429 of liposomes to kill H-1975 cell was followed as PSL > NL > CL. Therefore, AFT-loaded

430 PSL at concentrations less than 10 µM were performed in the next study.

431 3.9. Annexin-V apoptosis assay

432   Apoptosis-inducing influence of AFT loaded-PSL formulation was evidenced by

433   Annexin V/PI protocol. The extent and the nature of the induced cell death were analyzed

434   by flow cytometry. H-1975 cells were incubated with various concentrations of AFT

435   loaded-PSL (0.5 - 8 µM) for 24 h, which were selected based on WST-1 assay results. The

436   amounts of the early apoptotic and the late apoptotic cells, with necrotic cells were

437   determined after deduction of the proportion of spontaneous apoptosis. The results clearly

438   revealed that the AFT loaded-PSL triggered both apoptosis in H-1975 cells (Fig. 8A).

439   The quantities of apoptotic cells increased from 55 to 58.9 % after exposure to 0.5

440   to 1 µM of AFT loaded PSL. However, increasing the concentration to 8 µM resulted in a

441   reduction of the quantities of apoptotic cells from 30% at 3 µM to 9 % at 8 µM.

442   Furthermore, high cell viability of 87.5 % of free liposomes was observed. Concerning the

443   concentrations of AFT loaded-PSL at 3 to 8 µM, the proportions of necrotic cells increased

444   as the number of apoptotic cells decreased. The proportions of necrotic cells increased from

445   3 to 90%, depending on the concentrations of AFT loaded-PSL at 0.5 and 8 µM (a dose-

446   dependent manner) (Fig. 8B). Consequently, AFT at a concentration of 2.0 µM was

447   selected due to high apoptotic activity for further cytotoxicity studies using different lung

448   cancer cell lines.

449   Moreover, the cell viability of AFT loaded-PSL after H-1975 cells were incubated

450   for 48 and 72 h in addition to 24 h also was investigated (Fig. 9). The significant cytotoxic

451   effect in H-1975 cell at a concentration of 2 µM of AFT loaded-PSL, with the total cell

452   death proportion exceeding 78, 80 and 84 % after 24, 48 and 72 h, respectively. The

453   cytotoxic effect of the AFT-PSL formulation at a concentration of 2 µM was mainly due

454   to induced apoptosis, with slight necrosis. For comparison, the cell viability of free

455 liposomes at 72 h was 90 %. These results revealed that no significant difference in the cell

456 death after 24 and 48 h of exposure with H-1975 cells (p > 0.05). Therefore, 24 h of

457 exposure was selected for further study. Free liposomes showed insignificance cytotoxic

458 (apoptosis) after 24 and 48 h of exposure with considerable toxicity (necrosis) after 72 h

459 of exposure.

460 Overall, the obtained results clearly revealed the greater anticancer activity of PSL

461 as shown by a WST-1 assay and apoptosis assay. Therefore, 24 h of exposure was selected

462 for further cytotoxicity study of AFT-loaded PSL, CL and NL by using different lung

463 cancer cell lines. Hence, the anticancer activity of these liposomes was performed using

464 Flow cytometric analysis in the three cell lines as H-1975, H-1650, and HCC-827 (Fig.10

465 A, B & C). This study was conducted to detect the level of apoptosis induced after

466 incubation with various concentrations of 0.25, 0.5, 0.75, 1, and 2 µM of each liposomes

467 for 24 h. While, dimethyl sulfoxide and free liposomes were used as the controls. The

468 incubation of the cells with free liposomes did not induce notable cytotoxicity (data not

469 shown). The viability of H-1975 cells decreased more significantly compared to H-1650

470 and HCC-827 cells (p<0.05). PSL produced highest cytotoxic effect in the different lung

471 cancer cell lines (H-1975 cells and HCC-827) compared to NL and CL, when using

472 concentrations 2 µM AFT (Fig. 10). Overall, the results clearly revealed the superior

473 anticancer activity of PSL as shown by MTT assay and apoptosis assay.

474 **Discussion**

475 It has been reported that the cancer cells exhibited leaky vasculature with gap of

476 ~100 nm, this allows the drug to leak out of the blood vessels and into the cancer cells [29].

477 Additionally, cancer cells have an impaired lymphatic system; therefore, substances such

478   as drugs loaded-liposome can be retained for a relatively longer time [30]. This behavior

479   is commonly referred to EPR effect, which increases the exposure of tumor cells to drug

480   action. The liposomes have been reported as a potential carrier to target cancer cells. The

481   liposomes less 100 nm are able to escape the tumor vasculature and accumulate in the cells

482   by passive targeting [31]. Moreover, the targeted liposomes were designed depending on

483   the type of phospholipids used. In this study, it has been illustrated that modified liposomes

484   as PSL can work as an effective carrier for delivery of AFT *in vitro*. Moreover, this carrier

485   system presented significant antitumor activity. The desired liposomes can obtained by

486   investigating different quantities of the drug to lipid ratios to detect the greatest

487   encapsulated liposomes. Furthermore, the best liposomes in terms of vesicle size, PDI, ζ

488   and EE were selected. The *in vitro* release study and cytotoxicity of the selected liposomes

489   loaded AFT were examined. In addition, AFT is a potent antitumor drug used in clinical

490   oncology against a lung tumor. However, AFT had low specificity, systemic toxicity and

491   indiscriminating of the tumor and healthy tissues [14]. So AFT loaded-lipoosmes were

492   developed for successful cancer therapy that decreases dose-limiting toxicity. In this study,

493   a novel pH-sensitive liposomes-based AFT as targeted delivery (PSL) were used to target

494   tumor cells. It has been observed that PSL has intensely improved the cytotoxicity in

495   comparison to conventional liposomes (NL) or cationic liposomes (CL). Kraft *et al*

496   observed that CL or PSL could accumulate in the lung cells more, compared with NL [32].

497   PSL exposed to the destabilization behavior under acidic condition, which lead to rapid

498   release of its content. It is interesting that the tumor tissues are relatively acidic compared

499   to the normal tissue site [19-21]. The main difference between these two liposomes is the

500   composition of phospholipid used. In general, three lipid components: DSPC, DOPC, and

DOPE. DSPC were used. The rationale for the selection of DSPC was its stability against chemical degradation due to saturated lipid, which reduces the drug leakage from liposomes on storage and in vivo transit. To increase the fluidity of liposomal membrane, DOPC was selected due to its high fluidity at room temperature (transition temperature (T_m)= −20°C). While, T_m of DSPC is +55 °C, which remains in the gel phase [33]. Moreover, DOPE was combined to provide fusogenic characters to the liposomes, due to the formation of an inverted hexagonal phase upon destabilization of membranes at a mildly acidic pH [34]. Theses lipids possess various chain lengths and degrees of saturation, which can produce fine-tune the membrane dynamics and phase properties [35]. The main composition of CL is DOTAP, which is considered as a cationic phospholipid. While PSL composed from pH-sensitive phosphlipid (CHEMS). The film hydration method has been used to actively entrap AFT into liposomes with relatively high efficiencies and small vesicle size (<100 nm) [36]. The PDI values of the obtained liposomes are less than 0.3 indicating narrow size distribution. The higher ζ, of the obtained liposomes provoked the potential stability of a liposome. Patil *et al* investigated the influence of ζ on the cellular uptake of cerium oxide nanoparticles in A549 lung adenocarcinoma [37]. Thus, the charged surface of liposomes has ability to attach the cell membrane. Furthermore, to obtain the liposomes with the highest EE%, the best ratio of drug to phospholipid was selected for further studies. Accordingly, the highest EE% of AFT reached to 43.20%, 50.20%, and 52.01% for NL, PSL, CL, respectively at the 1:0.5 ratio of lipid to the drug. Nallamothu *et al* 2006 indicated that the high EE% of combretastatin A4 was obtained by increasing the drug to lipid ratios. By using 1:10 to 2:10 of combretastatin A4 to lipid ratios, the amount of the drug increased from 1.05 mg/ml

524 to 1.55 mg/ml, respectively. When the drug to lipid ratios was further increased to 4:10,

525 the EE% of the drug did not increase [38]. Thus, the best liposomes were subjected to

526 stability study, they exhibited better stability at 4°C or at 25°C after storage for 1 month.

527 CL showed the highest stability in term of EE%, particle size and zeta potential. This effect

528 is due to the inclusion of DOTAP in the liposomes, which decreases the rigidity of the

529 liposomes with good loading capacity. *In vitro* drug release data revealed that PSL and NL

530 exposed sustained release profiles due to the presence of DSPC (T_m), which lead to a

531 decrease in leakage of AFT in the circulation or extracellular environment. But in case of

532 CL, AFT exhibited high release rate compared with the other liposomes, at pH 7.4. This is

533 due to the complete protontion of DOTAP at pH 7.4 [39]. By contrast, the fast drug release

534 profile of AFT was found after addition PSL in acidic media, which reached to 100% after

535 4 h. The PSL undergoes destabilization at pH 5.5 and acquire fusogenic properties, thus

536 tended to rupture and quickly release of AFT. The fusogenic performance of PSL is due to

537 the presence of DOPE in the lipid layer, which forms a hexagonal structure instead of a

538 bilayer structure after dispersion in aqueous media. Düzgünes *et al* showed that liposomes

539 composed of CHEMS had high stabilize of EE calcein at pH 7.4 and undergo

540 destabilization and irreversible aggregation under acidic pH [40]. According to the kinetic

541 models, the release of AFT at pH 7.4 displayed release with Korsmeyer-Peppas model.

542 This effect is due to early rapid release followed by slow release of the liposomes [41]. In

543 case of the release pattern of PSL at pH 5.5, AFT release was quite faster with Korsmeyer-

544 Peppas model. This behaviour because AFT exists liposomal membrane, which leaks out

545 at a faster rate in acidic condition [42].

546   Therefore, it was confirmed that the pH-sensitive point in the liposome is close to

547   5 (the tumor microenvironment). PSL might release their content in the acidic environment

548   of the tumor tissues quickly. Therefore, the PSL were fabricated in the current study to

549   achieve a certain active targeting toward the tumor. The TEM of PSL revealed uniform,

550   homogenous and spherical-shaped liposomes with a smooth surface.

551   The potency of free AFT was compared with selected drugs depending on their

552   activity against lung cancer. The cell toxicity was evaluated by WST-1 using H-1975 cells.

553   The WST-1 assay showed that AFT is more effective as a cytotoxic agent compared to

554   other compounds used in lung cancer treatments (H-1975 cells). Furthermore, the anti-

555   proliferative effect of AFT on H-1975 cells was investigated at various concentrations for

556   24 h. The results indicated that the inhibition of cell viability AFT had concentration-

557   dependent manners. Moreover, anticancer activity of the obtained liposomes was also

558   investigated using and H-1975 cells. Unfortunately, WSR-1 assay failed to detect the

559   anticancer activity of the obtained liposomes due level of interference. However, a detailed

560   characterization of this interference was not undertaken here. Therefore, the levels of cell

561   viability between each liposomes were measured by using flow cytometry analysis after

562   Annexin V/PI staining. The results of flow cytometry after the treatment of cells with the

563   AFT loaded-PSL using different concentrations exhibited a comparable level of cell

564   intensity. It was clearly indicated that the uptake of AFT loaded-PSL by H-1975 cells was

565   higher than free AFT. The results revealed a marked decline in cell viability with AFT

566   loaded-PSL up to 60.4% of cell apoptosis at 1 µM after 24 h. The free AFT resulted in

567   apoptosis in 11.88% of the cells after 24 h. The low cytotoxic effect of free AFT could be

568   attributed to the low cellular uptake and poor trans-membrane permeability. Of the three

cancer cell lines tested, H-1975 cells appeared more sensitive to the liposomes. Particularly, the cytotoxicity of PSL is high compared with that of CL and NL. It is possible that PSL released AFT in response to the lowered pH in the endosome, and thus facilitated diffusion of the released AFT from the endosome to the cytosol. It has been suggested that pH-sensitive liposomes are internalized more efficiently than non-pH-sensitive formulations [43]. It is notable that the destabilization of PSL at the endosomal demonstrated that the efficacy of PSL depends on the pH of the tumor tissues [34]. Additionally, the liposomes containing CHEMS release their contents into the cytoplasm from 5 to 15 min upon their incubation with the cells [44]. The destabilization of PSL induced by acidification of the endosomal lumen represents the most important stage in the process of intracellular delivery. Carvalho *et al* developed cisplatin loaded-PSL to treat the SCLC. Compared with free cisplatin, the cytotoxicity of this PSL was significantly enhanced [7]. Kim *et al* developed a PSL with an efficient and targeted delivery system for gemcitabine, and represent a useful, novel treatment approach for tumors that overexpress EGFR [45]. More, the cationic liposomes containing paclitaxel composed of DOTAP were able to significantly decrease tumor perfusion and vascular diameter and the progress of A-Mel-3 melanoma in mouse models [46]. The association of cationic liposomes with surface membrane is due to the presence of anionic glycoproteins, such as sialic acid rich glycoproteins [47]. Furthermore, pH-sensitive liposomes containing cytarabine have been shown greatly antitumor effectiveness in both human HepG2 hepatoma cells and normal human liver L02 cells compared to non-pH-sensitive liposomes [48]. These promising results are required further *in vivo* analysis to understand the biodistribution profile of AFT loaded PSL to achieve new targeted-formulation for the tumor therapy.

4. Conclusion

In this work, a novel AFT-loaded PSL for targeted therapy of lung cancer (NSCLC) were developed. For comparison purpose, AFT-loaded NL, CL and PSL were successfully designed. The obtained liposomes showed small particle less than 100 nm with a low PDI (<0.27) and acceptable zeta potential with a spherical shape. The highest EE% values of the liposomes were achieved according the following order: CL>PSL>NL. The selected liposomes were stable at 4 and 25°C for 1 month. The PSL, CL and NL showed slow release profiles in pH 7.4. However, in acidic pH values, PSL exhibited fast release, which improved its tumor targetability. The selected liposomes revealed efficiency on cancer cells (NSCLC). Moreover, AFT-loaded PSL inhibited the cell growth of lung cancer cells more efficiently than free AFT, CL and NL based on using Annexin V assay. The obtained data indicate that AFT-loaded PSL is a promising a targeted drug delivery for cancer therapy.

Acknowledgements

References

1. Y. Bahader, and A.-R. Jazieh, Epidemiology of lung cancer, Ann. Thorac. Med. 3 (2008) 65-67.

2. O. Alamoudi, Prevalence of respiratory diseases in hospitalized patients in Saudi Arabia: A 5 years study 1996-2000, Ann. Thora. Med. 1 (2006) 76-80.

3. C.R. UK, Lung cancer and smoking. UK. Cancer Stats. Cancer Research UK. 2008. Sep., available form: http:// www.info.cancerresearchuk.org/cancerstats/ Lung/html.

617   4. K.A. Al-Turki, N.A. Al-Baghli, A.J. Al-Ghamdi, A.G. El-Zubaier, R. Al-Ghamdi,
618   Prevalence of current smoking in Eastern province, Saudi Arabia, East Mediterr. Health
619   J. 16 (2010) 671-667.

620   5. M.R. Davidson, A.F. Gazdar, B.E. Clarke, The pivotal role of pathology in the
621   management of lung cancer. J.Thorac. disease, 5 (2013) S463-S478.

622   6. A.Goel, S. Baboota, J.K. Sahni, J. Ali, Exploring targeted pulmonary delivery for
623   treatment of lung cancer. Int. J. Pharm. Invest. 3 (2013) 8-14.

624   7. T.C. Carvalho, S.R. Carvalho, J.T. McConville, Formulations for pulmonary
625   administration of anticancer agents to treat lung malignancies, J. Aerosol Med. Pulm.
626   Drug Deliv. 24 (2011) 61-80.

627   8. G. Pilcer, and K. Amighi, Formulation strategy and use of excipients in pulmonary
628   drug delivery, Int. J. Pharm. 392 (2010) 1-19.

629   9. S. Anabousi, U. Bakowsky, M. Schneider, H. Huwer, M. Lehr, C. Ehrhardt, In vitro
630   assessment of transferrin-conjugated liposomes as drug delivery systems for inhalation
631   therapy of lung cancer, Eur. J. Pharm. Sci. 29 (2006) 367-374.

632   10. T. Mukohara, Mechanisms of resistance to anti-hu C man epidermal growth factor
633   receptor 2 agents in breast cancer, Cancer Science, 102 (2011) 1-8.

634   11. G.Metro, and L. Crinò, The LUX-Lung clinical trial program of afatinib for non-small-
635   cell lung cancer, Expert rev. anticancer ther. 11 (2011) 673-682.

636   12. F. Solca, G. Dahl, Z. Aoephel, G Bader, M. Sanderson, K. Clein, O. Kraemer, F.
637   Himmelsbach, E. Haaksma, G.R. Adolf, Target binding properties and cellular activity
638   of afatinib (BIBW 2992), an irreversible ErbB family blocker, J. Pharmacol. Exp. Ther.
639   343 (2012) 342-350.

640   13. V. Hirsh, Afatinib (BIBW 2992) development in non-small-cell lung cancer, Future
641   Oncology 7 (2011) 817-825.

642   14. S.C. Coelho, G.M. Almeida, M.C. Pereira, F.S. Silva, Functionalized gold
643   nanoparticles improve afatinib delivery into cancer cells, Expert Opin Drug Deliv, 13
644   (2016) 133-41.

645   15. Y. Malam, M. Loizidou, A.M. Seifalian, Liposomes and nanoparticles: nanosized
646   vehicles for drug delivery in cancer, Trends Pharmacol sci. 30 (2009) 592-599.

647   16. S. Martins, B. Sarmento, D.C. Ferreira, E.B. Souto, Lipid-based colloidal carriers for
648   peptide and protein delivery-liposomes versus lipid nanoparticles, Int. J. nanomedicine,
649   2 (2007) 595-607.

650   17. A.S. Ulrich, Biophysical aspects of using liposomes as delivery vehicles, Bioscience
651   reports 22 (2002) 129-150.

652   18. T. Liu, H. Choi, R. Zhou, I.W. Chen, RES blockade: A strategy for boosting efficiency
653   of nanoparticle drug, Nano Today, 10 (2015) 11-21.

654   19. Y. Duan, L. Wei, J. Petryk, T.D. Ruddy, Formulation, characterization and tissue
655   distribution of a novel pH-sensitive long-circulating liposome-based theranostic
656   suitable for molecular imaging and drug delivery, Int. J. Nanomedicine 11 (2016)
657   5697-5708.

658   20. M. Chang, S. Lu, F. Zhang, T. Zuo, Y. Guan, T. Wei, W. Shao, G. Lin, RGD-modified
659   pH-sensitive liposomes for docetaxel tumor targeting, Colloids Surfaces B 129 (2015)
660   175-182.

661   21. Y. Zhang, Y. Wang, Y. Yang, S. Liu, Q. Ruan, X. Zhang, J. Tai, T. Chen, High tumor
662   penetration of paclitaxel loaded pH sensitive cleavable liposomes by depletion of tumor
663   collagen I in breast cancer, ACS Appl. Mater. Interfaces 7 (2015) 9691-9701.

664   22. S.S. Guan, J. Chang, C.C. Cheng, T.Y. Luo, C.C. Wang, S.H. Liu, Afatinib and its
665   encapsulated polymeric micelles inhibits HER2-overexpressed colorectal tumor cell
666   growth in vitro and in vivo, Oncotarget. 5 (2014) 4868-4880.

667   23. Y. Fan, C. Chen, Y. Huang, F. Zhang, G. Lin, Study of the pH-sensitive mechanism of
668   tumor-targeting liposomes, Colloids Surf. B Biointerfaces, 151 (2017) 19-25.

669   24. S. Dash, P.N. Murthy, L. Nath, P. howdhury, Kinetic modeling on drug release from
670   controlled drug delivery systems, Acta Pol. Pharm. 67 (2010) 217-23.

671   25. R. Vejendla, C. Subramanyam, G. Veerabhadram, New RP-HPLC method for the
672   determination of afatinib dimaleate in bulk and pharmaceutical dosage forms, Indo-
673   American J. Pharmaceut. Res. 5 (2015) 2015-2111.

674   26. F. Meng, R. Cheng, C. Deng, Z. Zhong, Intracellular drug release nanosystems,
675   Materials Today, 15 (2012) 436-442.

676   27. Y. Zhao, W. Ren, T. Zhong, S. Zhang, Tumor-specific pH-responsive peptide-modified
677   pH-sensitive liposomes containing doxorubicin for enhancing glioma targeting and
678   anti-tumor activity, J. Controlled Rel. 222 (2016) 56-66.

679   28. N.A. Peppas, J.J. Sahlin, A simple equation for the description of solute release. III.
680   Coupling of diffusion and relaxation, Int. J. Pharm.57 (1989)169-172.

681   29. H.M. Mansour, C.-W. Park, D. Hayes, Nanoparticle lung delivery and inhalation
682   aerosols for targeted pulmonary nanomedicine. 2013: CRC Press, Taylor & Francis
683   Group: Boca Raton, FL, USA.

684   30. H. Maeda, H. Nakamura, J. Fang, The EPR effect for macromolecular drug delivery to
685   solid tumors: Improvement of tumor uptake, lowering of systemic toxicity, and distinct
686   tumor imaging in vivo, Adv. drug deliv. Rev. 65 (2013) 71-79.

687   31. M. Brandl, Liposomes as drug carriers: a technological approach, Biotechnol Annual
688   Rev. 7 (2001) 59-85.

689   32. J.C. Kraft, J.P. Freeling, W. Zang, R.J. Ho, Emerging research and clinical
690   development trends of liposome and lipid nanoparticle drug delivery systems. J Pharm.
691   .Sci. 103 (2014) 29-52.

692   33. A. Fahr, P. van Hoogevest, S. May, B.Nergstrand, S. Leigh, Transfer of lipophilic
693   drugs between liposomal membranes and biological interfaces: consequences for drug
694   delivery, Eur. J. Pharm. Sci. 26 (2005) 251-265.

695   34. R. Karanth, R.S. Murthy, pH-Sensitive liposomes-principle and application in H.cancer
696   therapy, J. Pharm. Pharmacol. 59 (2007) 469-483.

697   35. U. Michaelis, H. Haas, Targeting of cationic liposomes to endothelial tissue, in
698   Liposome Technology, G. Gregoriadis, Editor. 2006, Informa Healthcare, 151-170.

699   36. G.M. Jensen, T.H. Bunch, Conventional liposome performance and evaluation: lessons
700   from the development of Vescan, Journal of liposome research, 17(2007) 121-137.

701   37. S.Patil, S. Aandberg, E. Heckert, W. Self, S. Seal, Protein adsorption and cellular
702   uptake of cerium oxide nanoparticles as a function of zeta potential, Biomaterials, 38
703   (2007) 4600-4607.

704   38. R. Nallamothu, G.C. Wood, K.F. Kiani, L.A. Thoma, A targeted liposome delivery
705   system for combretastatin A4: formulation optimization through drug loading and in
706   vitro release studies, PDA J. Pharm. Sci. Technol, 60 (2006) 144.

707 39. N.J. Zuidam, Y. Barenholz, Electrostatic and structural properties of complexes
708   involving plasmid DNA and cationic lipids commonly used for gene delivery, Biochim
709   Biophys Acta, 1368 (1998) 115-128.

710 40. J.J. Sudimack, W. uo, R.J. Lee, A novel pH-sensitive liposome formulation containing
711   oleyl alcohol, Biochim Biophys Acta, 1564 (2002) 31-37.

712 41. C. Koutsoulas, N. Pippa, C. Demetzos, M. Zabka, Preparation of liposomal
713   nanoparticles incorporating terbinafine in vitro drug release studies J. Nanosci.
714   Nanotechnol. 14 (2014), 4529-4533.

715 42. S. Modi, B.D. Anderson, Determination of drug release kinetics from nanoparticles:
716   overcoming pitfalls of the dynamic dialysis method, Mol. Pharm. 10 (2013), 3076-
717   3086..

718 43. T. Ishida, Y. Okada, H. Kiwada, Development of pH-sensitive liposomes that
719   efficiently retain encapsulated doxorubicin (DXR) in blood, Int. J. Pharm. 309(2006)
720   94-100.

721 44. D.S. Collins, K. Findlay, C.V. Harding, Processing of exogenous liposome-
722   encapsulated antigens in vivo generates class I MHC-restricted T cell responses, J.
723   Immunol. 148 (1992) 3336-3341.

724 45. I.-Y Kim, Y.S. Kang, D.S. Lee, H.J. Park, E.K. Choi, Y.K. Oh, J.S. Kim, Antitumor
725   activity of EGFR targeted pH-sensitive immunoliposomes encapsulating gemcitabine
726   in A549 xenograft nude mice. J. Controlled Rel. 140 (2009) 55-60.

727 46. S. Strieth, M.E. Eichhorn, B. Sauer, B. Schulze, M. Teifel, U. Michaelis, M. Dellian,
728   Neovascular targeting chemotherapy: encapsulation of paclitaxel in cationic liposomes
729   impairs functional tumor microvasculature, Int. J. Cancer 110, (2004)117-124.

730 47. R. Weijer, M. Broekgaarden, M. Kos, R. van Vught, E.A. Rauws, E. Breukink, T.M.
731   van Gulik, G. Storm, M. Heger, Enhancing photodynamic therapy of refractory solid
732   cancers: combining second-generation photosensitizers with multi-targeted liposomal
733   delivery, J. Photochem. Photobiol. Chem. 23 (2015) 103-131.

734 48. L. Wang, D. Geng, H. Su, Safe and efficient pH sensitive tumor targeting modified
735   liposomes with minimal cytotoxicity, Colloids Surf B Biointerfaces 123 (2014) 395-
736   402.

737

738 **Table 1**

739 Compositions of different types of liposomes.

Phospholipids*	Amount required (µmol/mL)		
	NL	PSL	CL
DSPC	3	3	3
DOPC	10	7	7
DOPE	3	3	3
CHEMS	-	3	-
DOTAP	-	-	3

740
741 *NL: Non-targetin liposomes; CL: Cationic liposomes; PSL: pH-sensitive liposomes;
742 DSPC: 1,2-distearoyl-sn-glycero-3-phosphocholine[18:0]; DOPC: 1,2-dioleoyl-sn-
743 glycero-3-phosphocholine [18:1]; DOPE:1,2-dioleoyl-sn-glycero-3-phosphoethanolamine
744 [18:1]; CHEMS: Cholesteryl hemisuccinate; DOTAP:1,2-dioleoy-3-trimethylammonium-
745 propane Chloride salt (DOTAP)
746

747

748

749

750

751

752

753

754

755

756

757

758

759

760

761

Table 2

Precision of the developed method for analysis of AFT.

Nominal (µg/mL)	Concentrations Mean ± SD	CV%
0.01	0.01 ± 6.09	0.9266
0.05	0.05 ± 6.40	0.8051
0.1	0.1 ± 5.71	1.7143
0.25	0.25 ± 1.76	0.7076
0.5	0.5 ± 5.70	1.1404
1	1 ± 1.77	0.1763
2	2 ± 4.03	2.3016
5	5 ± 5.65	1.0731
10	10 ± 3.76	1.3577
20	20 ± 3.83	0.1992
25	25 ± 2.55	0.1102

764

765   SD: standard deviation; CV: Coefficient of variation percetage

766

767

768

769

770

771

772

773

774

775

Table 3

Repeatability for different levels of AFT (n = 3).

Concentration (µg/ml)	Mean ± SD[a]	Precision RSD[b] (%)	Accuracy (%)
Inter day			
0.1	99.98 ± 1.98	1.98	99.9
1	1000.72 ± 0.49	0.05	102
10	10000 ± 113.26	1.13	100.1
Intra-day			
0.1	100 ± 1.06	1.07	99.86
1	1000 ± 0.29	0.03	100.5
10	10000 ± 60.08	0.6008	100.2

a   Standard deviation of the mean
b   Relative standard deviation

780

781

782

783

784

785

786

787

788

789

790

791

792

793

794

795

Table 1

Release kinetics of AFT release from different liposomes.

pH media	Codes	Zero order	First order	Higuchi (Diffusion)	Korsmeyer Peppas	"n" value
	CL	0.691	0.559	0.871	0.940	0.460
pH 7.4	NL	0.928	0.731	0.988	0.994	0.681
	PSL	0.754	0.634	0.912	0.971	0.431
pH 5.5	PSL	0.647	0.486	0.835	0.889	0.599

798

799

800

801

802

803

804

805

806

807

808

809

810

811

812

813

Table 5

Drug release kinetics parameters derived from Korsmeyer Peppas.

pH media	Codes	$^a n_1$	$^a k_1$	$^b n_2$	$^b k_2$
	CL	0.675	16.987	0.168	37.619
pH 7.4	NL	0.681	3.606	0.527	5.434
	PSL	0.483	8.809	0.201	16.381
pH5.5	PSL	0.941	20.910	0.181	59.671

816

^{a}The first stage is 0-4 h. ^{b}The second stage is 6-24 h.

818

819

820

821

822

823

824

825

826

827 **Fig. 1**

828

829
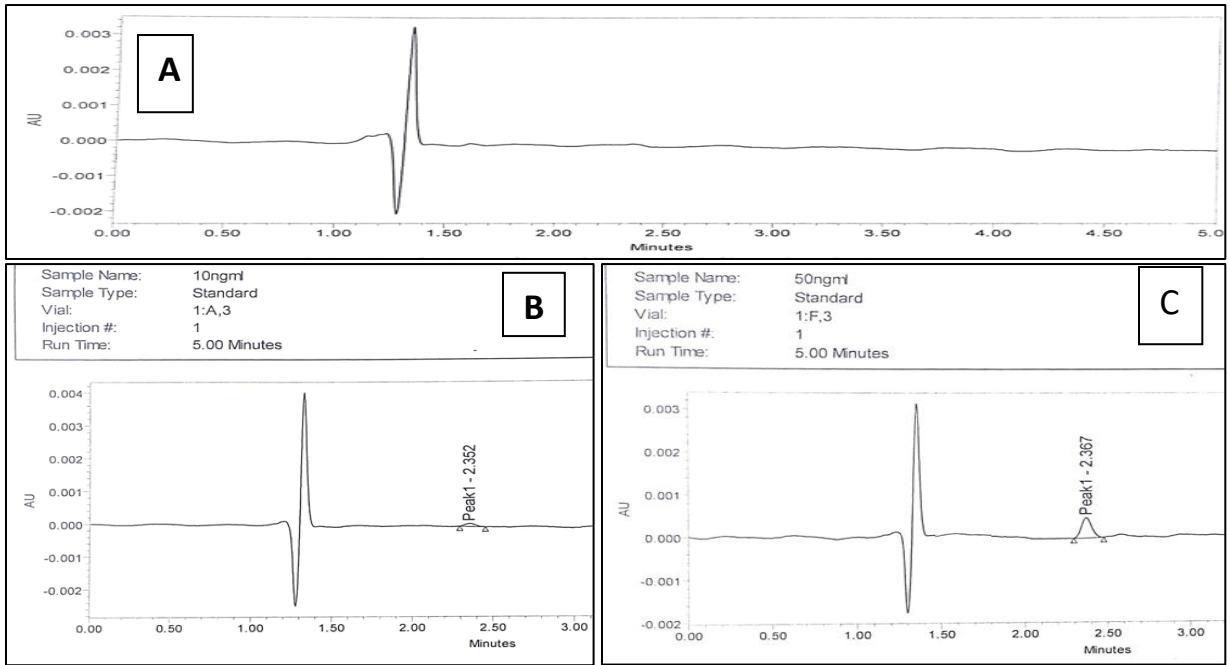
Fig. 1. HPLC chromatograms of the mobile phase (chromatogram A), and HPLC chromatograms of the mobile phase containing (B) 10 ng/ml and (C) 50 ng/ml afatinib.

830

831

832

833

834

835

836

837

838

839 **Fig. 2**

840
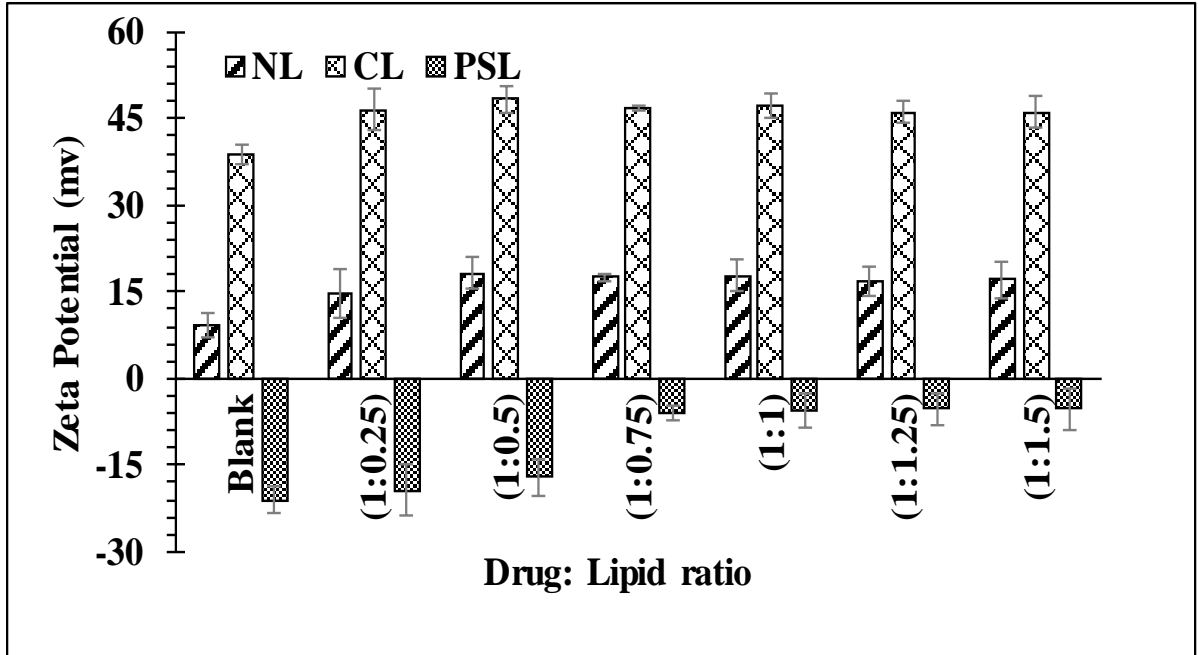
Fig. 2. Zeta potentials of afatinib-loaded liposomal formulations at different lipid to drug ratios.

841

842

843

844

845

846

847

848

849

850

851

852   **Fig. 3**
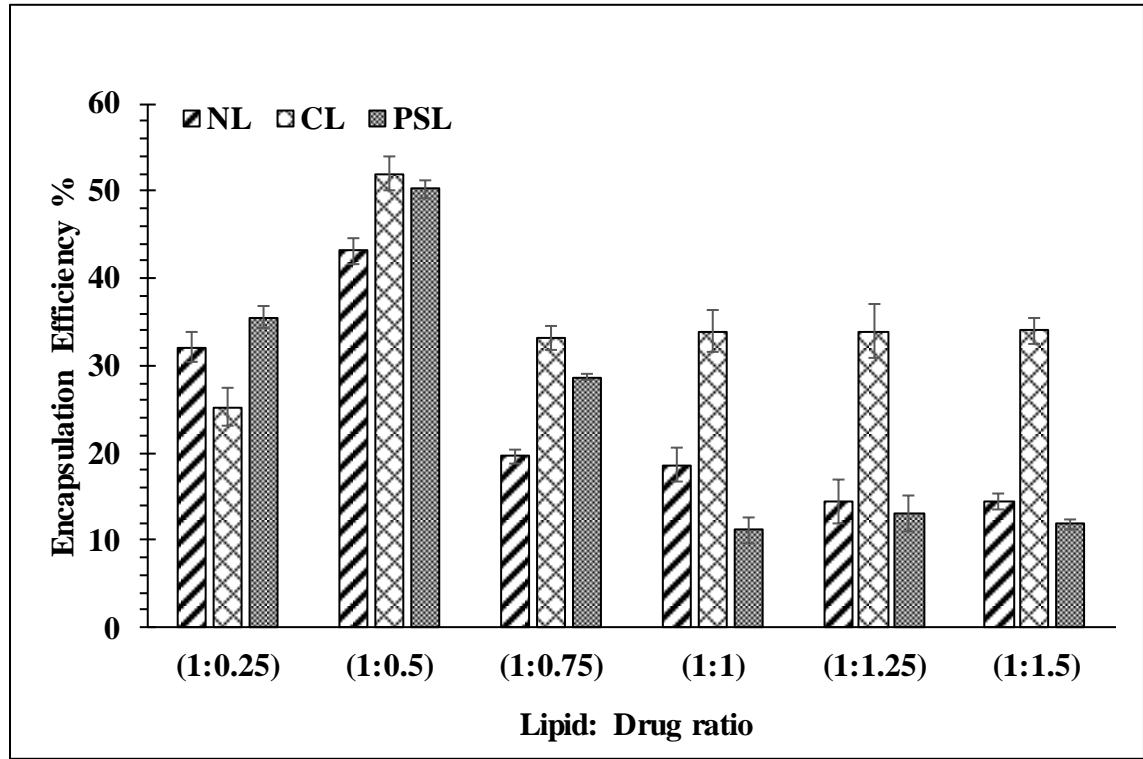
Fig. 3. EE% of afatinib-loaded different liposomal formulations with different lipid to drug ratios.
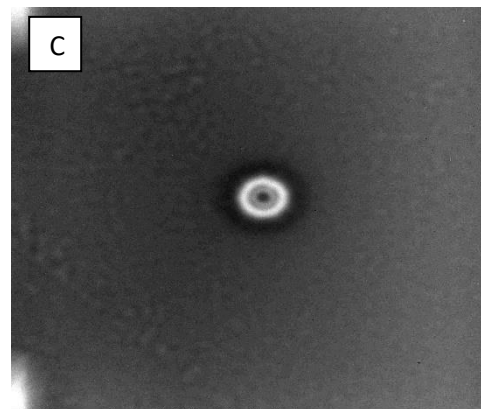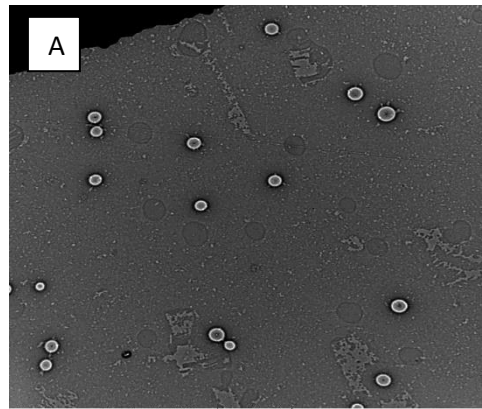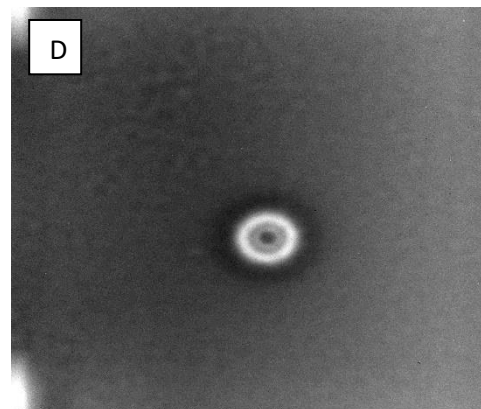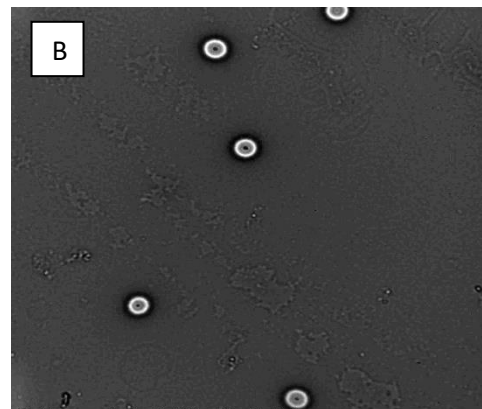
Fig. 4

Fig. 4. TEM micrographs of the pH sensitive liposome at a drug to lipid ratio of 1:0.5 (PSL), using varied magnification power.

Fig. 5

901

902

903

904

905

906

907

908

909

910

911
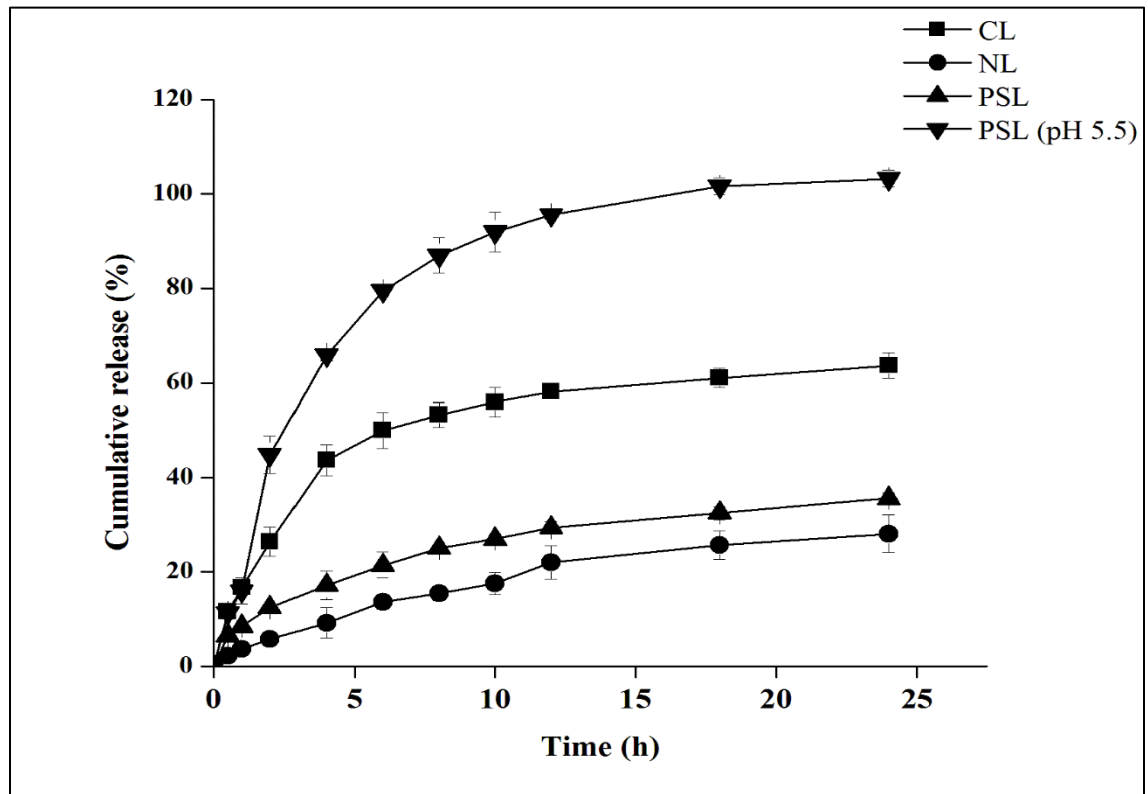
Fig. 5. *In vitro* release profiles of the liposomal formulations loaded with afatinib in phosphate-buffered saline containing 0.2% Tween 80 at pH 7.4 and pH 5.4. Values are presented as the mean ± SD.

912

913

914

915

916

917

918

919

920

921   **Fig. 6**

922
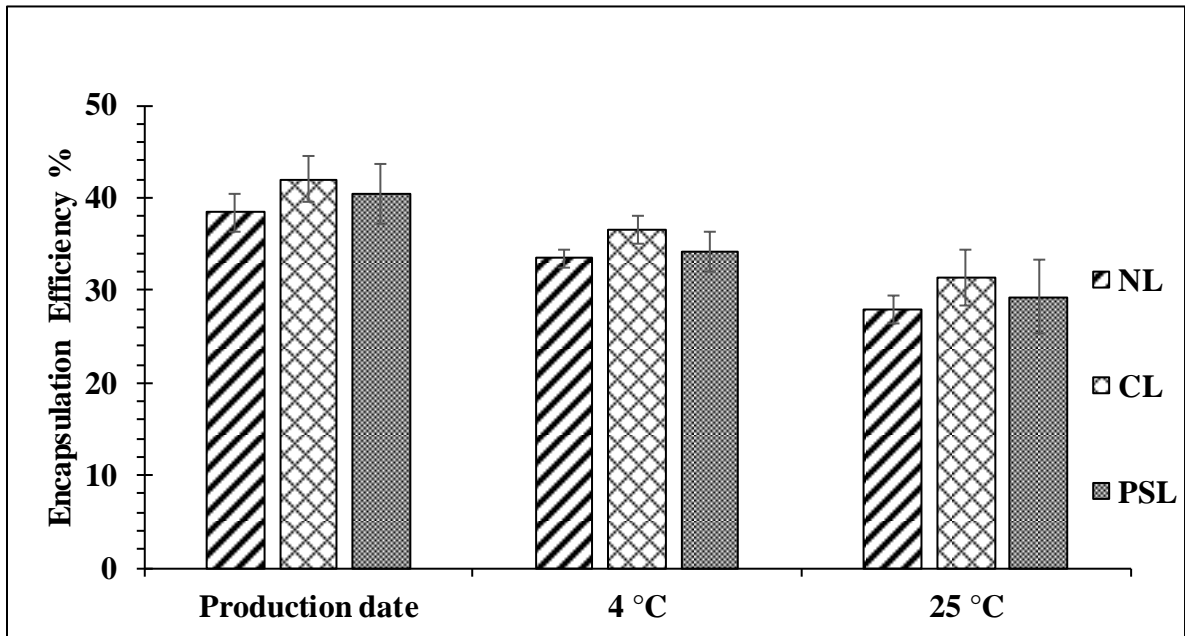
Fig. 6. EE % of afatinib at the ratio 1:0.5, following storage for one month at 4 and 25°C, of NL (nontargeting liposome), PSL (pH sensitive liposome) and CL (cationic liposome), P = 0.141.

924

925

926

927

928

929

930

931   **Fig. 7**

932

933

934

935

936

937

938

939

940

941

942
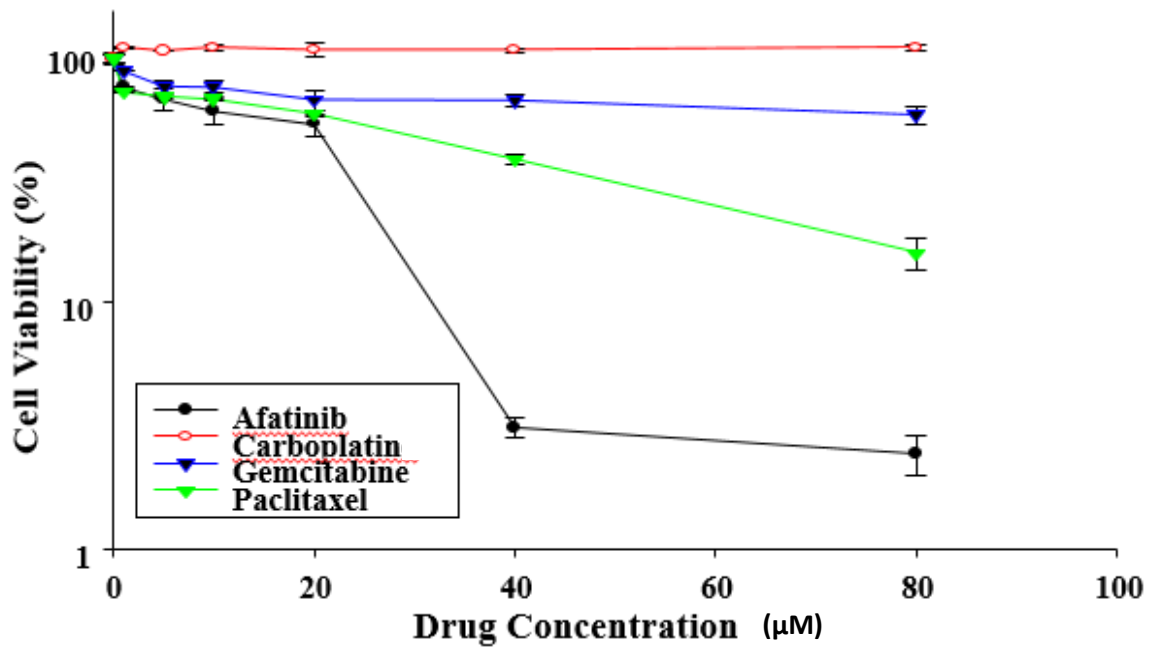
Fig. 7. Cytotoxicity of afatinib, carboplatin, gemcitabine and paclitaxel on H-1975 cells, as
943 determined by a WST-1 assay. Cells were treated with varying concentrations of the drugs for
24 h. Results are from three independent experiments and are expressed as the mean ± SD.

944

945

946

947

948

949

950   **Fig. 8**

951
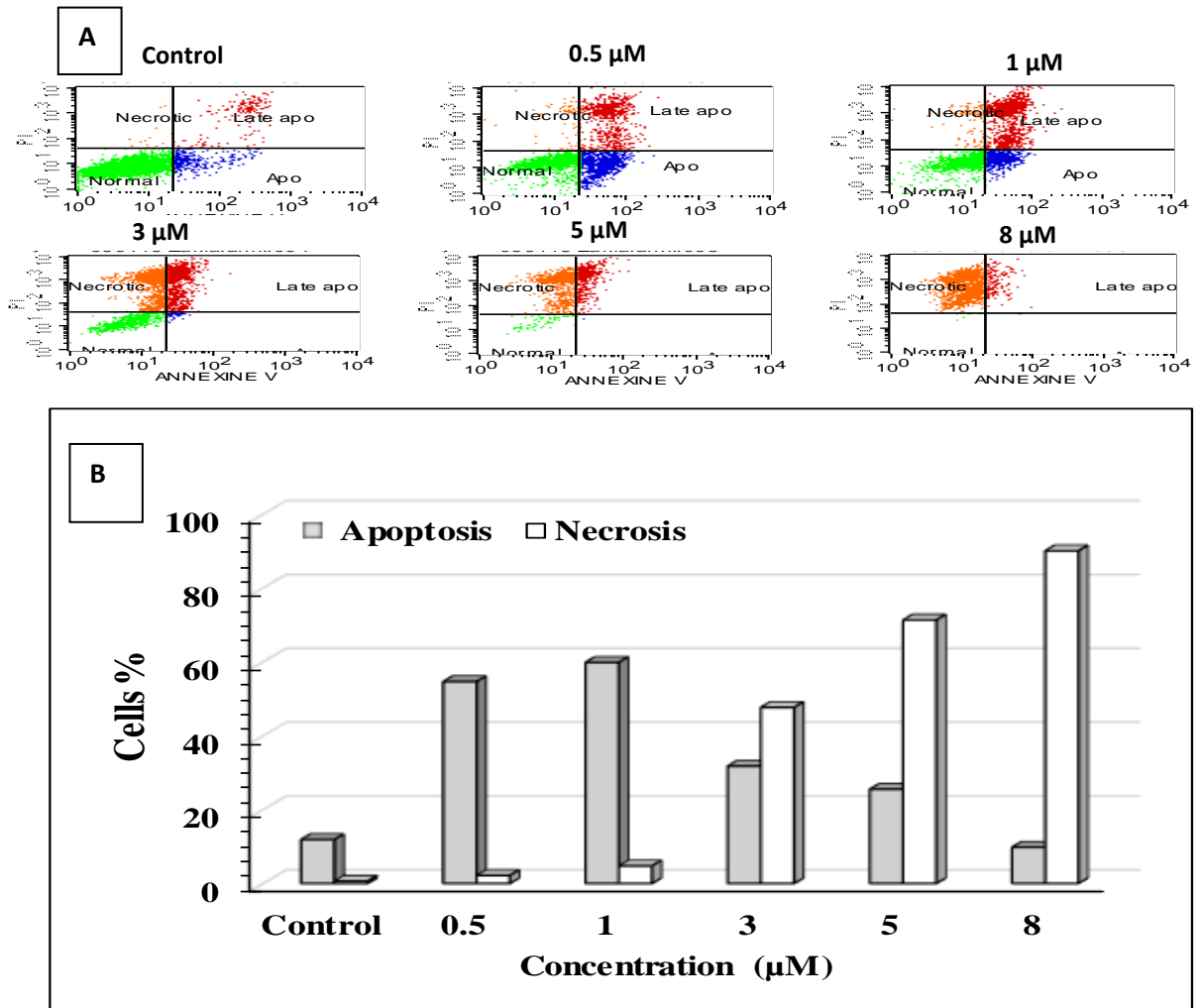
Fig. 8. H-1975 lung cancer cells were either treated with free liposomes, as controls, or challenged with Afatinib loaded liposomes (PSL2) for 24 hrs, and then the proportion of apoptosis and necrosis was analysed by Annexin V/PI-flowCytometry. four groups of cells, viable cells that excluded both Annexin V and PI (Annexin V/PI), bottom left; early apoptotic cells that were only stained with Annexin V (Annexin V+/PI), bottom right; late apoptotic cells that were stained with both Annexin V and PI (Annexin V+/ P+), top right and necrotic cells that were only stained with PI (Annexin V/PI+), top left. (A) Flow charts. (B) Histogram showing the percentage of induced apoptosis in H-1975cells.

953

954

955
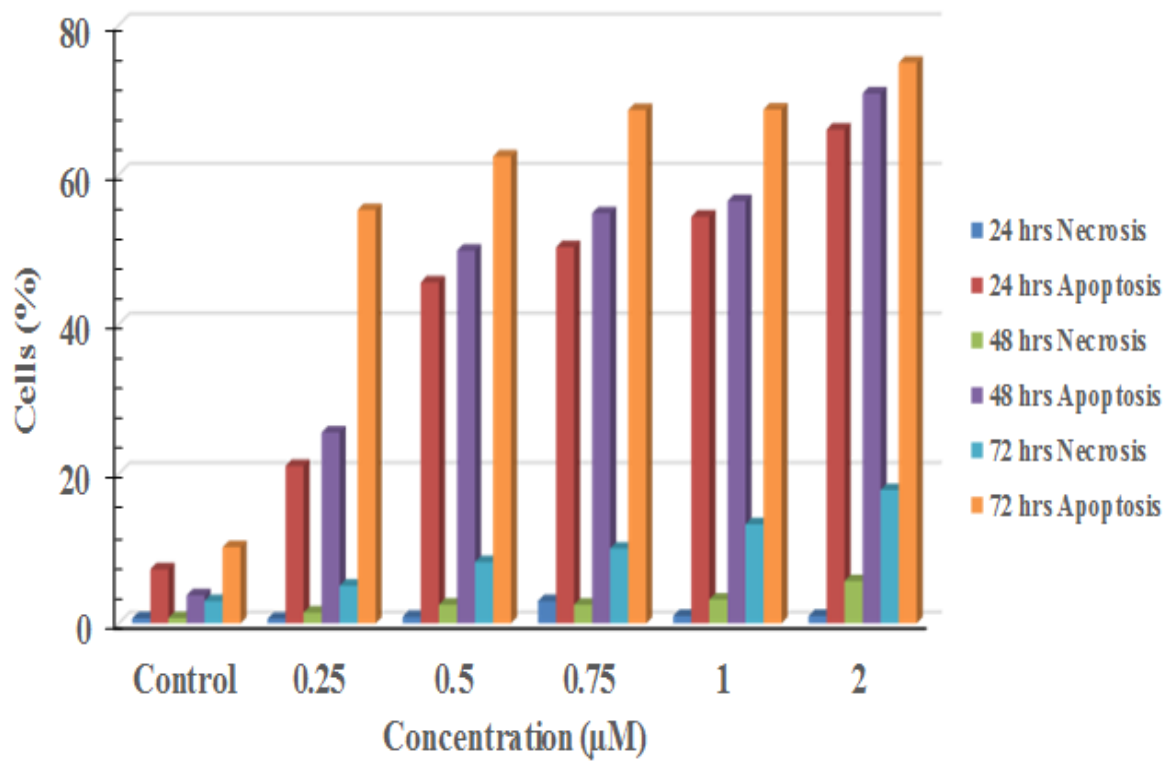
Fig. 9

Fig. 9. H-1975 cells were challenged with pH-sensitive liposomes (PSL) (0.25-2 µM) for 24, 48 or 72 h, following which apoptosis was analysed with Annexin V/PI-flow cytometry. Each value represents the mean ± SD of three independent experiments performed in triplicate.

Fig. 10

967

968

969

970

971

972

973

974

975

976

977

978
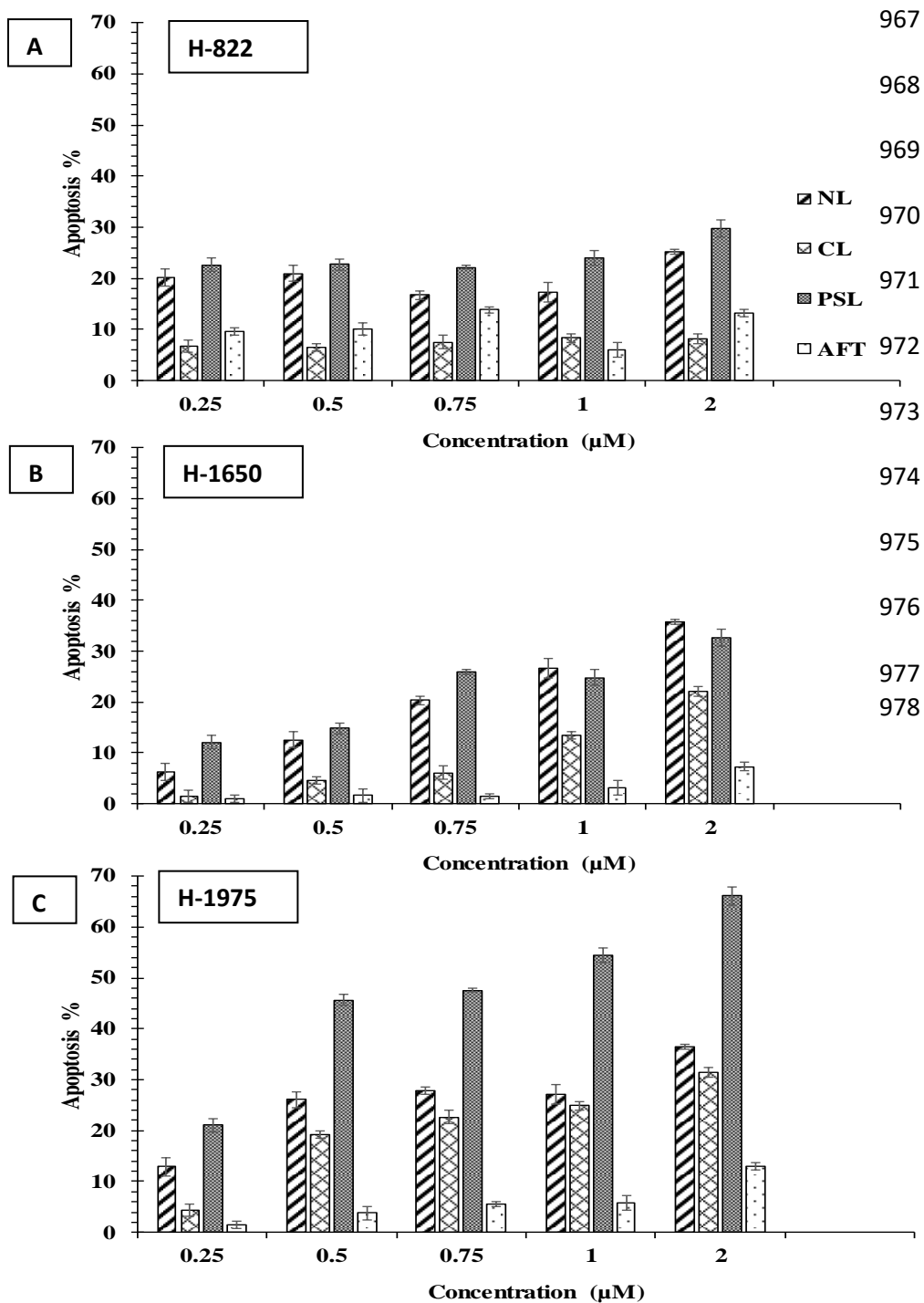
Fig.10. Non-small cell lung cancer cells were either treated with Blank Liposomes, as control, or challenged with AFT and AFT-loaded liposomes (PSL, NL, CL) for 24 h, following which the proportion of apoptotic cells was analysed using Annexin V/PI-flow cytometry. Histogram shows the percentage of induced apoptosis in H-1975 cells. Each point represents the mean ± SD of three independent experiments performed in duplicate.